Parametric Bottom-Up Cost Modelling of Tidal Energy Converters for Site-Specific Feasibility Studies

M. Petri, E. Gorr-Pozzi*, M. Corrales-González, and G. Giorgi

Marine Offshore Renewable Energy Lab (MOREnergy Lab), Department of Mechanical and Aerospace Engineering (DIMEAS), Politecnico di Torino, Corso Duca degli Abruzzi 24, 10129 Turin, Italy; petri.mattia00@gmail.com (M.P.); manuel.corrales@polito.it (M.C.-G.); giuseppe.giorgi@polito.it (G.G.)

* *Correspondence: emiliano.gorr@polito.it (E.G.-P); Tel.: +52-1-646-108-9712*

Abstract

Tidal energy represents a promising yet underexploited source within the marine renewable sector, offering predictable and sustainable generation potential that aims to increase interest in offshore energy alternatives. This study presents a detailed bottom-up techno-economic optimization assessment model adapted to tidal energy converter (TEC) systems. The novelty model breaks down component-level costs for TECs into three foundational types: gravity-based substructures (GBS), floating platforms, and monopiles. Unlike traditional top-down methods, the model couples these foundation-specific costs with site-specific tidal resource data to evaluate energy yield and economic performance. The model is applied to five different locations, i.e., Fall of Warness (UK), Fromveur and Raz Blanchard (France), Punta Pezzo (Italy), and Cozumel (Mexico), to assess how local bathymetry, tidal velocities, and distance to shore affect the feasibility of the TEC plant. Validation against real-world data from the ATIR floating platform project shows strong agreement with actual deployment costs and performance. Results from the case studies indicate that monopile and floating TECs typically achieve higher capacity factors and lower Levelized Costs of Energy (LCoE) compared to GBS systems. The monopile configuration is more suitable for shallow water, while floating platforms prove more cost-effective in deep-water sites. By highlighting the importance of tailoring TEC configurations with specific site conditions, these insights provide a robust and scalable tool for informing early-stage design and policy-making.

Keywords: Marine renewable energy, tidal energy, levelized cost of energy,

cost reduction, electricity market, bottom-up approach.

1. Introduction

Increasing pressure to reduce fossil fuel consumption and mitigate climate change has accelerated the expansion of renewable energy systems [1]. However, land availability and conflicts with agriculture and urban development limit further onshore deployment, increasing costs in land acquisition. Offshore renewable technologies offer a promising alternative due to the vast extent of marine areas, higher and more stable wind and current resources, and reduced visual impact [2]. Among them, tidal energy provides additional benefits such as high predictability, limited surface footprint, and consistent energy production [3, 4].

Despite their potential, Marine Renewable Energy (MRE) technologies, such as Tidal Energy Converter (TEC) and Wave Energy Converter (WEC), remain at early deployment stages [5]. Their commercialization is hindered by low learning rates, limited operational experience [6], and the scarcity of detailed techno-economic data. Existing cost models often rely on the Top-down Approach (TdA), which allocates total project cost across high-level components [5], offering limited flexibility in assessing alternative device configurations. Bottom-up Approach (BuA) estimates the cost of each sub-component, enabling more detailed and scalable evaluations. However, their application to tidal technologies is still limited. To date, only one BuA model exists [7], but it lacks sufficient detail and adaptability for practical use. The present work addresses this gap by developing a comprehensive parametric BuA cost functions for TEC systems.

Tidal currents arise from periodic water level variations influenced by bathymetry and coastal geometry, with stronger flows in constrained channels [4]. High-velocity sites include Saltstraumen (up to 10 m/s), Pentland Firth ($>$2.5 m/s) [8], and Fall of Warness (up to 4 m/s) [9]. Tidal energy benefits from water's high density, yielding greater energy per unit volume than wind, and predictable cycles enabling up to 20 h/day of generation and grid stability [10]. TECs are broadly classified into tidal range and tidal stream technologies. Tidal stream systems, which extract kinetic energy from currents, are the focus of this work. Among them, Horizontal Axis Turbines (HATs) are the most mature, reaching TRL 8–9 with rated powers between 100 kW and 2 MW, while alternatives such as tidal kites are at TRL 7–8 [4]. HATs can be deployed using different foundation systems [11]:

- Gravity-Based Substructures (GBS) approach employs massive structural foundations that maintain seabed positioning through frictional forces generated by their substantial weight, typically composed of steel or concrete.

- Monopile foundations utilize drilled seabed penetration techniques, analogous to offshore wind installations, and can accommodate dual TEC units mounted on adjustable crossarms that enable operational flexibility for maintenance procedures.

- Floating platform systems utilize seabed-anchored mooring arrangements with heavy anchor systems, supporting dual TEC units positioned beneath the platform to capture energy from elevated water column flows.

Available economic data show substantial variability between tidal energy configurations. For GBS installations, capital expenditure (CapEx) is estimated at 3.65 M€/MW with operational expenditure (OpEx) of 0.18 M€/MW for a 40 MW deployment [12]. Floating platform configurations present lower capital requirements, with industry projections indicating costs of 2.6 M£/MW (CapEx) and 0.20 M£/MW (OpEx) for 10 MW arrays [13]. In contrast, monopile systems demonstrate higher capital requirements; the MeyGen Phase 1C development (73.5 MW capacity) projects investment costs of 6.8 M€/MW, although operational cost data for this configuration remain unavailable [14]. Performance data from UK installations indicate an average capacity factor (CF) of 29.9% for GBS systems [15]. Reported Levelized Cost of Electricity (LCoE) values for tidal stream technologies range between 0.11–0.48 €/kWh, with current estimates of 0.125 €/kWh for floating TEC systems [16] and projections of 0.10 €/kWh by 2030 as deployment scales increase [4].

Commercialization of tidal energy faces strong competition from mature technologies such as wind and solar; therefore, supportive policy frameworks and long-term deployment programs remain essential [17]. TECs may play an important role especially in remote or island communities, where they can enhance energy independence and reduce fossil fuel reliance [18], stimulating economic growth through job creation and reduced energy costs.

The work presented in this paper addresses a clear gap in the existing literature by developing a systematic bottom-up techno-economic modelling framework for the three main HATs configurations, applied to five potential case studies. The novelty of this work lies in building a parametric, data-driven methodology that systematically models and links sparse techno-economic information to a continuous representation of costs across different technologies, rated powers, and installation sites, thereby supporting sustainability-oriented techno-economic assessments. Tidal resource availability, energy production, and cost metrics are quantitatively evaluated and compared against available literature data.

The remainder of the paper is structured as follows: Sect. 2 presents the materials and methods, including study areas, the state of the art of BuA, the tidal resource and power assessment, and the techno-economic assessment; Sect. 3 presents and discusses system performance and competitiveness across sites; and Sect. 4 provides the summary and main conclusions of the research.

2. Methods

This study conducts a comprehensive techno-economic feasibility assessment across five distinct locations, evaluating three TEC foundation technologies: Gravity-Based Substructure (GBS), monopile, and floating platform configurations. The analysis integrates site-specific environmental parameters with TEC technical specifications to determine total project costs through the developed cost model. Subsequently, power generation estimates are derived by applying device-specific power curves to local tidal resource characteristics, enabling the calculation of key techno-economic performance indicators. The complete analytical framework, from input parameters to final outputs, is illustrated in Figure 1.

2.1. Study areas

The study focuses on five distinct marine locations selected for their potential in tidal energy exploitation. These sites were chosen based on the availability of tidal current data, existing tidal energy projects, and their diversity in geographical characteristics: the Fall of Warness (Scotland), Fromveur and Raz Blanchard (France), Punta Pezzo (Italy), and Cozumel (Mexico). The selected sites differ significantly in terms of tidal current velocity, water depth, and proximity to shore, encompassing both nearshore, easily accessible locations and deeper offshore conditions. Fall of Warness is characterized by high tidal velocities (up to 4 m/s [9]), making it an established reference locations for device testing and commercial array development. Raz

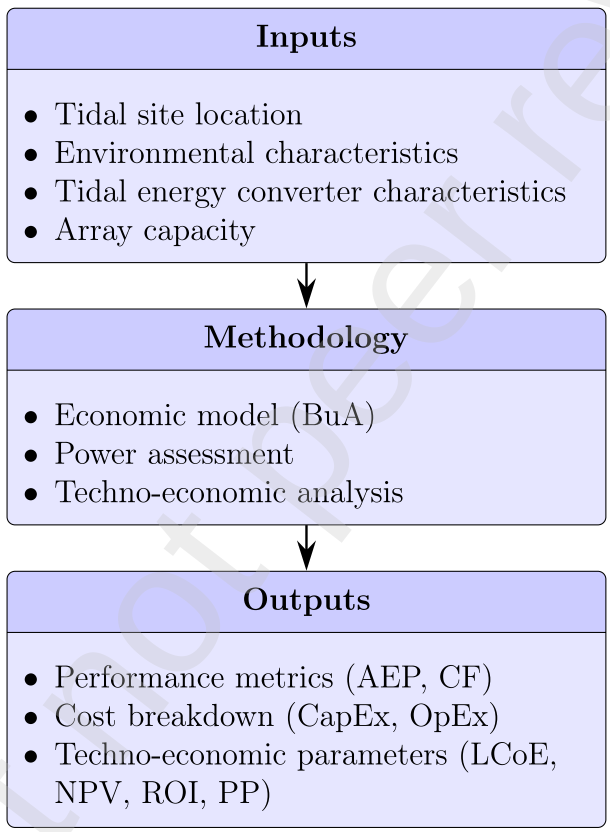

Figure 1: Workflow of the techno-economic tidal model.

Blanchard exhibits exceptional tidal currents due to the constriction between Alderney Island and Cap de la Hague [19], with depths of approximately 55 m at 11 km from shore. Fromveur provides comparable flow intensity at moderate depths, with particular interest for local off-grid power supply to Ushant Island [20]. Punta Pezzo, in the Strait of Messina, combines strong currents ($\approx$3 m/s) with greater depths ($\approx$100 m), offering logistical advantages due to its coastal proximity [21]. Finally, the Cozumel channel in Mexico represents the shallower and highly accessible case in this study ($\approx$19 m) [1]. Detailed site descriptions are provided in the Supplementary Material.

These locations were chosen based on accessible tidal data availability, as direct measurements via Acoustic Doppler Current Profilers (ADCPs) present substantial financial constraints [22].

2.2. State-of-the-art bottom-up approach

Cost estimation methodologies for technological development can be categorized into two approaches: the Top-down Approach (TdA) and the Bottom-up Approach (BuA). TdA starts from the total project cost and allocates percentages to major system components based on historical data. Although simple to apply, it offers limited insight into how design parameter variations affect component-level costs due to its aggregated structure. Conversely, BuA disaggregates the system into individual subcomponents and technical parameters, enabling the development of detailed cost functions and reducing estimation uncertainty [5]. While TdA provides a high-level perspective, BuA yields more accurate and configuration-specific estimates, although it requires extensive technical data and is less suited to early design stages. Few cost functions specifically designed for TECs are available in the literature. Due to high similarity with wind turbines, many wind turbine component cost functions have been adapted for TEC applications when validity ranges are satisfied. To address this literature gap, this study presents the first comprehensive BuA cost model specifically developed for tidal energy systems, enabling detailed techno-economic comparison of three TEC foundation technologies across five diverse tidal sites and providing technology-specific economic insights through parametric cost functions tailored to marine environments.

2.3. Assessment of tidal energy resource

One of the most significant advantages of tidal energy is its high predictability, which follows regular cycles, making precise forecasting of tidal currents and energy generation possible. Due to the high costs of ADCPs, real measurement datasets were not publicly available, but only statistical result or a single value was provided, so four different cases of tidal energy resource assessment were provided to present different methodologies in data usage.

1. Model data and bias correction: Tidal velocity data are retrieved from the Global Ocean Physics model provided by the Copernicus Marine Service [23]. The dataset is subsequently corrected using available field measurements, specifically the annual average velocity $Uz_{mean} = 1.5$ m/s recorded by the ATIR floating platform at a rotor depth of z = 13.9 m [16]. To assess current speeds at the depth of interest, a power law equation is applied, expressed as (1),

$$U(z) = U_{mean} \cdot \left(\frac{h - z}{\beta \cdot h}\right)^{\frac{1}{\alpha}} , \tag{1}$$

   where the bed roughness β=0.4 and power law exponent α=7 are given parameters from the study that proposed the equation [24], while U_{mean} is the depth-averaged velocity, h is the water depth, and z is the rotor depth. This equation is later used in all case studies.

2. Tidal current time series: in this case, a dataset from the DTOceanPlus project database was retrieved [25], obtained from the HOMERE model developed by Ifremer, using an unstructured grid, and already validated with ADCP measurements [25].

3. Tidal current harmonic analysis: In this case, the harmonic components of the tidal current were provided. Specifically, an ADCP measurement campaign was conducted at the site of interest over a 24-day period. A time-domain harmonic analysis was then carried out, allowing the tidal stream velocity to be estimated as the superposition of sine functions [26].

4. Yearly current frequency analysis: In this case, the use of numerical models such as the Copernicus dataset is not appropriate. This is mainly due to the model's low spatial resolution, which makes it unsuitable for accurately capturing rapid bathymetric variations and the dynamics occurring near the shoreline. Therefore, data for this site

were retrieved from the literature. The available data consist of the yearly relative frequency of the depth-averaged current velocity V_{mag}, derived from ADCP measurements [1]. For this specific case, a different, yet comparable, power law velocity profile is used, as it was directly provided together with the velocity data. The vertical velocity distribution is defined as (2),

$$U(z) = U_{mean} \cdot (h - z)^{\frac{1}{b}} \ , \tag{2}$$

where the power law exponent is b=6.14. The depth-averaged velocity is expressed as

$$V_{mag} = \frac{\int_h^0 U(z)dz}{h} \tag{3}$$

2.4. Extractable tidal power

TEC power curves are implemented to estimate the amount of extractable tidal power based on the annual tidal resource dataset, as defined in (4),

$$P = \frac{1}{2}\rho A \, C_p U^3 \,, \tag{4}$$

where ρ is the water density, set to 1025 kg/m^3, A is the rotor swept area, Cp is the power coefficient, and U is the tidal current speed. Each turbine operates within a specific range of velocity, generating power from the cut-in speed (U_{in}) to the cut-out speed (U_{out}), and delivering rated power (P_{rated}) between the rated speed (U_{rated}) and U_{out}.

Based on the derived tidal power dataset, the annual energy production (AEP) and capacity factor (CF) can be computed [27].

In this analysis, it is assumed that all generated power is transmitted to the onshore substation without accounting for losses through the generator or export cables. In addition, wake effects are neglected, and as a result, the CF value is considered independent of the TEC array configuration.

2.5. Techno-economic assessment

This study adopts a techno-economic assessment approach for TECs, in which the overall capital cost is evaluated through a modular cost breakdown based on the primary subsystems of the device. Each subsystem is associated with a specific cost function that reflects the corresponding design parameters, allowing for scalable and flexible cost estimation across different configurations. The main input variables and assumed parameters are listed in

Table 1, together with their respective typical ranges of values. A complete list of cost functions related to each TEC component is reported in Tables S1, S2 and S3. Only Development Expenditures (DevEx) were assumed to be 5% of total CapEx without using a BuA [28]. Additionally, nacelle cover cost is considered 21% of nacelle cost (rotor + PTO + yaw system) as derived from the case study in [7].

Some cost functions require input parameters not previously defined, such as the thrust coefficient C_T (used to evaluate the thrust force F_T), low-speed shaft angular velocity ω_{lss} (B.4) and the tip-speed ratio (TSR), set to 4.5 for three-bladed [29] and 6.0 for two-bladed turbines [30].

The assumed values of cost metrics and parameters used in this analysis were retrieved from real tidal energy projects and used as inputs to the corresponding cost functions.

Steel price represents a critical parameter in foundation cost estimation and must be selected according to application-specific requirements. For floating platforms, a steel price of 2.5 €/kg was adopted to reflect the high-quality materials and fabrication requirements typical of offshore structures. The mooring system employs lower-grade steel at 0.5 €/kg, consistent with chain and anchor manufacturing standards. Monopile foundations utilize A36 structural steel, priced at 1.2 €/kg by incorporating an 80% mark-up over base material costs to account for processing and fabrication [31]. GBS structures employ a cost of 0.8 €/kg, reflecting the use of lower-grade steel primarily for ballast purposes, with pricing positioned between raw steel commodity rates [32] and structural steel costs.

Installation costs represent a significant component beyond equipment manufacturing, encompassing turbine substructure, turbine assembly, electrical infrastructure, and mooring system deployment. These costs primarily depend on installation duration and vessel specifications, with rates varying substantially among different vessel types. The general installation cost function for turbines and substructures can be expressed as,

$$\begin{aligned} C_{inst} &= \frac{N}{N_{trip}} \left(t_{inst} + 2\frac{d}{V_{vessel}} \right) C_{vessel} \\ &= \frac{N}{N_{trip}} \left(t_{inst} + 2\frac{d}{V_{vessel}} \right) (C_{rent} + C_{fuel}) \ , \end{aligned} \tag{5}$$

where N represents the total number of elements to be transported, N_{trip} is the number of elements per trip, d/V_{vessel} is the transit time based on port

Table 1: Main input variables of the BuA-based cost model, with typical ranges of values and assumed values for some parameters

Parameter	Symbol	Value	Units
Water depth	h	—	/
Distance to the shore	d	—	/
No. of blades	N_{blades}	2—6	/
Rated current	U_{rated}	2—4.5	m/s
Rotor diameter	D	5—24	m
Rated power	P_{rated}	100—2000	kW
No. of turbines per structure	$N_{turb,sub}$	1 or 2	/
No. of structures	N_{sub}	array dep.	/
Export voltage	V_{export}	11—33	kV
No. of export cables	$N_{cable,exp}$	array dep.	/
No. of rows for array	N_{row}	array dep.	/
No. of columns for array	N_{column}	array dep.	/
Output voltage from generator/array voltage	V_{array}	0.69	kV
Power factor	PF	0.95	/
Gearbox ratio	i	1/98	/
Thrust coefficient	C_T	0.9	/
Ratio of cover and rotor diameter	D_{cover}/D	0.1333	/
Floating platform mass	$M_{platform}$	360	tons
Anchor weight	M_{anchor}	140	tons
Chain diameter	D_{chain}	0.076	m
Steel price for mooring	$P_{steel,mooring}$	0.5	€/kg
Steel price for floating platform	$P_{steel,platform}$	2.5	€/kg
Steel price for GBS	$P_{steel,GBS}$	0.8	€/kg
A36 steel price for monopile	$P_{steel,mono}$	1.2	€/kg
Monopile outer diameter	D_{out}	3.5	m
n° mooring lines	$n_{mooring}$	4	/

distance and vessel speed, t_{inst} is the on-site installation time, and C_{vessel} encompasses vessel rental costs, depending on type of vessel and domain of validity of cost variable (see Table S4 [33]), and fuel cost. Environmental factors affecting vessel operations are not modeled due to their complexity and site-specific variability. Additionally, 3 workers are assumed to be on each vessel, with a cost rate of 50 €/h. [5].

The installation time represents the remaining variable needed to complete Equation (5), and all the installation phases' durations are detailed in Table S5.

Within the installation cost framework, the workers' cost for onshore elements ($N_{elements}$) preparation is evaluated based on a crew of 6 workers, with each element requiring 1 hour of preparation time.

For clarity and computational efficiency, the power cable installation cost was estimated following the methodology of [34], assuming one-third of the cable is buried beneath the seabed (282 €/m) and two-thirds are surface-laid (100 €/m).

OpEx comprises all operational and maintenance expenses incurred throughout the plant's operational lifetime, with maintenance activities predominantly executed during suitable weather windows. These costs are conventionally divided into maintenance operations and insurance coverage [7]. The evaluation of maintenance costs presents significant challenges due to their strong dependency on maritime and weather conditions. While many studies quantify OpEx as a fraction of CapEx or per unit of installed capacity, these methodologies cannot adequately reflect the cost variations arising from different system configurations. Although comprehensive modeling frameworks coupled with statistical analysis would provide the most accurate OpEx assessment, the present study prioritizes computational simplicity while preserving reasonable cost estimation accuracy. Consequently, maintenance costs are determined through consideration of annual failure rates of key components, associated spare parts expenses (set at 15% of the original component cost), and required repair durations (see Table S6) [35]. Given the absence of specific repair time data for floating and monopile configurations in the available literature, these values were estimated by applying a 30% time reduction compared to the corresponding GBS TEC repair schedules. Insurance costs are also included in OpEx, assumed to be 1% of CapEx, which aligns closely with findings from the Meygen project [36].

Decommissioning costs (D_c) refer to the expenses associated with the removal of the tidal plant at the end of its operational life. These costs depend on the type of TEC foundation, as different removal techniques and vessel specifications are necessary, (see Table S7) [37].

2.6. Cost function adjustments

The cost functions and datasets used in this analysis originate from different studies spanning various years, regions, and currencies. To enable consistent economic comparison, all costs were adjusted using the Consumer Price Index (CPI), which accounts for inflation over time and across regions. Economic data were normalized to 2024 values (CPI_{2024}) for each country and expressed in euros for consistency. Each reference cost was scaled according to the corresponding $CPI_{reference,year}$, following the CPI-based adjustment provided in Equation (B.7) [38], with CPI data summarized in Table S8.

2.7. Techno-economic parameters

The evaluation of different TEC configurations requires a robust techno-economic framework. Several financial indicators are employed to estimate plant profitability and feasibility, including the Levelized Cost of Energy (LCoE), Net Present Value (NPV), Return on Investment (ROI), Payback Period (PP), and the amount of avoided CO_2 emissions E_{CO_2}. All techno-economic parameter equations are reported in Appendix B. The discount rate r was assumed to be equal to 5%, and the project lifetime n=25 years [16].

LCoE, NPV, ROI, and PP were calculated according to equations provided in Appendix B, assuming constant annual revenues (R_t) and OpEx over the project lifetime. Electricity revenues were evaluated using an electricity selling price p_{el}=207 €/MWh, consistent with UK tidal energy support schemes [39]. The environmental benefit was quantified through E_{CO_2}, calculated using an emission factor EF of 532 g $CO_{2,eq}$/kWh, representative of electricity production from natural gas [40].

3. Results and discussion

This section presents the outcomes of the techno-economic analysis based on the developed BuA model. First, the model is validated against real-world data from the ATIR floating tidal platform to assess its accuracy and consistency with existing project costs. Secondly, the validated model is applied to five selected sites to evaluate and compare the performance and economic feasibility of different TEC configurations under varying environmental conditions.

3.1. Cost model validation through ATIR floating TEC

To validate the proposed cost model, a real-world case study was analyzed: the ATIR floating tidal platform, developed by Magallanes Renovables and deployed at the EMEC test site in Scotland [41]. Platform characteristics and cost data were collected from technical literature and public sources (see Tables S9 and S10). The export cable was excluded from the model since the ATIR platform was directly connected to EMEC's infrastructure.

Table 2 presents the capital expenditures (CapEx) and operational expenditures (OpEx) estimated by the cost model versus the real costs of the ATIR tidal platform provided by Magallanes Renovables [42].

Most of the cost categories align closely between the model and the real project. Larger deviations are observed in the control and auxiliary components, which include the power converter and wet-mate connectors, respectively. These discrepancies may be present due to outdated cost references or project-specific supply chain conditions. For example, the power converter was reassigned to the control category instead of electrical to better reflect its role and to avoid overestimation.

A significant deviation was found in the mooring material cost. Based on the known mooring system mass and reported project cost, a steel price of approximately 0.26 €/kg would be required to match the real expense. This value is unrealistically low compared to current raw steel prices. Thus, the cost model used 0.5 €/kg, which is consistent with the cost of raw steel [32]. While the total OpEx estimation is reasonably close, the breakdown was not fully available from the developer, so direct comparison of individual components is not possible.

A single case study validation is insufficient to ensure model reliability, necessitating comparison with additional projects of different TEC types. The Meygen project, comprising four fixed tidal turbines in Scotland's Pentland Firth, represents one of the earliest commercial tidal developments [36]. However, direct cost comparison proves challenging due to the project's pioneering nature. As one of the world's first large-scale tidal arrays, Meygen encountered significant risks associated with unproven technology, resulting in elevated insurance premiums and contingency costs. The fractured rock seabed and extreme tidal forces required custom engineering solutions for cable stability, further inflating project costs. Additionally, operational expenses were dominated by lease payments and insurance costs, reflecting the high-risk profile of early-stage tidal energy deployment. Consequently, Mey-

Table 2: CapEx and OpEx comparison between model results and real project data

Component	Model Cost [€]	Real Cost [€]
Platform	**2,801,801**	**2,876,562**
Structure	900,000	912,787
Mechanical	911,900	1,217,391
Electrical	360,779	327,244
Control	231,538	102,448
Auxiliary	270,808	123,258
Blades	126,777	193,434
Installation	**654,377**	**519,169**
Mooring Design	—	10,000
Mooring materials	374,238	200,000
Cable	107,576	106,830
Installation	113,681	83,339
Transport	44,801	100,000
Blade installation	14,080	19,000
Engineering (DevEx)	**181,904**	**158,747**
Design	—	100,909
Construction	—	57,838
Total CapEx	**3,638,083**	**3,554,478**
Maintenance	89,656	—
Insurance	36,377	—
Total OpEx	**126,033**	**96,000**

gen's costs substantially exceed both the floating platform case study and the present cost model results, limiting its utility for model validation.

Despite only one real case study having been analyzed, meaning the ATIR floating TEC, the model can be considered validated by existing data because the Meygen project couldn't represent nowadays costs and knowledge of tidal energy, and no additional real cost data is available in the literature.

3.2. Application of the techno-economic model to selected tidal sites

The application of the techno-economic model to selected tidal locations yields various results and techno-economic metrics, which are better listed in Table A.5, and the main insights derived from it are briefly discussed below. Water depth ranges from 19 to 100 meters, with deeper locations such as Punta Pezzo experiencing reduced energy production and increased installation costs for the GBS configuration. Similarly, greater distances from shore, such as the 11 km distance at Raz Blanchard, result in higher power export cable costs, as well as installation and maintenance procedures.

The capacity factor (CF) is computed for each location, with floating and monopile configurations achieving higher values compared to GBS TEC systems, as well as higher annual energy production (AEP). This improved performance results from the higher positioning of the rotor relative to the seabed, which enables the extraction of stronger current velocities and optimizes turbine operation. The exception is Cozumel, where the tidal plant operates in shallow water depths. In this case, the GBS rotor must be positioned higher to satisfy the minimum clearance constraint of 6 m between the blade tip and seabed [43]. Additionally, different minimum clearance requirements must be met between the blade tip and sea level: 8 m for GBS configuration and 4.4 m for floating and monopile configurations [44]. Conversely, Punta Pezzo exhibits the lowest CF due to its significant depth, which forces the GBS TEC to operate at considerably lower velocities compared to surface currents, thereby limiting the turbine's operational potential.

Table 3 presents the techno-economic results for the maximum array size considered in this study (32 turbines) which was chosen due to the natural trend of LCoE reduction as the array capacity increases, as later demonstrated in Figure 4. This corresponds to 32 MW for Fall of Warness, Fromveur, and Raz Blanchard, 19.2 MW for Punta Pezzo, and 3.3 MW for Cozumel. The latter two locations exhibit lower array capacity due to less powerful turbines, as detailed in Table A.5. Cozumel exhibits the lowest OpEx due to its proximity to shore, in contrast to Raz Blanchard, which incurs higher costs due to its distance from land. Most case studies demonstrate profitability, with exceptions being the GBS configuration at Punta Pezzo and all configurations at Cozumel. The unprofitability at Cozumel stems from reduced energy production caused by the less powerful TEC, whose diameter is constrained by shallow water depth, and the site's lower energy resource. In most cases, the monopile TEC achieves the lowest LCoE, except at Punta Pezzo, where high water depth increases foundation costs, making the floating TEC more economically viable. Conversely, GBS consistently shows the lowest profitability across all locations, except at Cozumel, where shallow water depth favors GBS and monopile configurations over floating systems. It should be noted that the floating platform mass and mooring system design are assumed constant in this analysis; in reality, shallow depths and lower currents would reduce both mass and costs.

Table 3: Techno-economic assessment results for different configurations

Parameter	**Fall of Warness**	**Fromveur**	**Raz Blanchard**	**Punta Pezzo**	**Cozumel**
GBS configuration					
Installed Power [MW]	32	32	32	19.2	3.296
Capacity Factor [%]	26.17	31.83	20.24	9.76	12.3
AEP [MWh]	73444	89142	56793	16427	3554
CapEx [M€]	97.93	100.6	128.9	57.58	24.25
OpEx [M€]	2.02	2.01	2.41	1.11	0.398
LCoE [€/MWh]	124.9	104.9	207.0	328.9	653.1
NPV [M€]	85.01	128.3	0.006	-28.22	-22.35
ROI [%]	65.77	97.33	0.004	–	–
PP [years] †	10	8	24	–	–
E_{CO_2} [t_{CO_2eq}] ‡	39072	47423	30214	8739	1891
Floating configuration					

Techno-economic assessment results for different configurations (continued)

Parameter	Fall of Warness	Fromveur	Raz Blanchard	Punta Pezzo	Cozumel
Installed Power [MW]	32	32	32	19.2	3.296
Capacity Factor [%]	33.24	39.35	28.49	20.83	11.51
AEP [MWh]	93066	110166	79891	35040	3325
CapEx [M€]	64.15	74.77	126.6	48.56	30.56
OpEx [M€]	1.60	1.78	2.99	1.09	0.577
LCoE [€/MWh]	66.7	64.8	150.5	131	840.9
NPV [M€]	184.1	220.8	63.64	37.51	-29.7
ROI [%]	210.6	219.4	37.56	57.97	—
PP [years] †	5	5	13	11	-–
E_{CO_2} [t_{CO_2eq}] ‡	49511	58608	42502	18641	1769
Monopile configuration					
Installed Power [MW]	32	32	32	19.2	3.296
Capacity Factor [%]	33.24	39.35	28.49	20.83	11.51
AEP [MWh]	93066	110166	79891	35040	3325
CapEx [M€]	47.98	68.24	117.9	57.85	14.78
OpEx [M€]	1.24	1.64	2.81	1.24	0.27
LCoE [€/MWh]	52.6	61.1	143.1	159.8	396.5
NPV [M€]	202.5	226.5	71.99	23.29	-12.45
ROI [%]	293.6	238.6	44.69	29.51	—
PP [years] †	3	4	12	14	–
E_{CO_2} [t_{CO_2eq}] ‡	49511	58608	42502	18641	1769

† PP: Payback Period
‡ E_{CO_2}: Environmental impact of decarbonization

In Figure 2 the CapEx distributions for Punta Pezzo and Raz Blanchard

Table 4: Comparison of main techno-economic results and literature values

TEC	Tidal site	CF [%]	CapEx [M€/MW]	OpEx [M€/MW]	LCoE [€/MWh]
GBS	A	26.17	3.06	0.24	124.87
	B	31.83	3.14	0.20	104.90
	C	20.24	4.03	0.37	206.99
	D	9.76	3.00	0.59	328.88
	E	12.3	24.25	0.98	653.09
	Benchmark [12]	**29.9**	**3.65**	**0.18**	**100 [4]**
Floating	A	33.24	2.00	0.15	66.65
	B	39.35	2.34	0.14	64.82
	C	28.49	3.96	0.33	150.48
	D	20.83	2.53	0.27	131.04
	E	11.51	7.36	1.52	840.93
	Benchmark [13]	**29.9**	**3.12†**	**0.234†**	**100**
Monopile	A	33.24	1.50	0.12	52.59
	B	39.35	2.13	0.13	61.14
	C	28.49	3.69	0.31	143.06
	D	20.83	3.01	0.31	159.83
	E	11.51	9.27	0.71	396.45
	Benchmark [14]	**29.9**	**6.8**	**–**	**100**

A=Fall of Warness, B=Fromveur, C=Raz Blanchard, D=Punta Pezzo, E=Cozumel

† Currency conversion of 1£ = 1.2€(January 2025)

are represented for a 32-turbine array, whose tidal sites were selected for high water depth and large distance from shore, respectively. As observed from the pie charts, foundation cost represents the predominant contribution at Punta Pezzo, since the high water depth increases both monopile height and mooring system length, while GBS remains unaffected by this environmental parameter. At Raz Blanchard, power cable cost represents the main contribution to CapEx due to the large distance from shore, except for the GBS configuration, in which the offshore substation allows for a single high-capacity export cable, increasing costs only slightly compared to a nearshore location. Conversely, installation costs are elevated due to the large distance, resulting in longer transit times to reach the tidal plant. Figure 3 reports the ROI and NPV for these two sites. GBS configurations do not yield a positive return, with the Raz Blanchard GBS TEC achieving only marginal profitability (ROI = 0.004%). In contrast, both floating and monopile configurations show increasing profitability as the array size increases.

As already observed in Table 4, Fromveur proved to be the most convenient tidal site for a TEC array installation. For this convenient location, the LCoE trend is reported in Figure 4. The results demonstrate that increasing turbine array capacity leads to a reduction in LCoE values. This trend is most pronounced for GBS TECs, where export cable cost savings become more significant as the turbine number increases. Contrary, floating and monopile TECs exhibit only marginal LCoE reductions because each foundation incorporates its transformer, requiring individual export power cables per foundation. However, this LCoE monotonic decrease may be altered when environmental constraints are explicitly incorporated into the optimization framework. With their inclusion, the optimal configuration often features fewer turbines than the solution that maximizes power output alone. This suggests that the incorporation of site-specific environmental restrictions could result in an optimal array size with a minimum LCoE at intermediate capacities rather than at maximum deployment scales [45].

Returning to the case studies techno-economic results, Fall of Warness and Fromveur achieve CF values close to the UK average (29.9%), while other locations show suboptimal performance due to insufficient resources or mismatched technology, as shown in Table 4. The LCoE targets set by the JRC are only met at Fall of Warness and Fromveur using floating or monopile systems. GBS TECs, representing first-generation devices [15], fail to achieve LCoE below 100 €/MWh due to higher CapEx and OpEx. Literature cost estimates vary significantly and sometimes conflict. The model confirms that

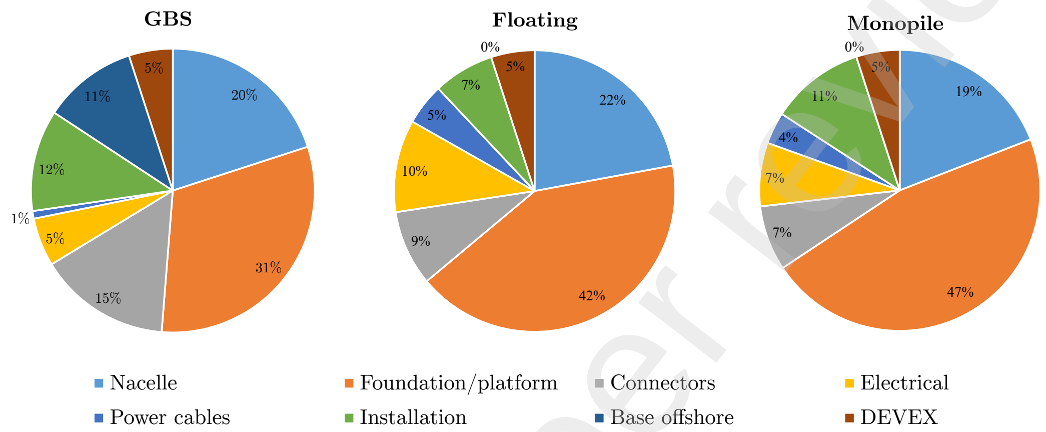

(a) CapEx distribution for 32 TEC array (19.2 MW) in Punta Pezzo.

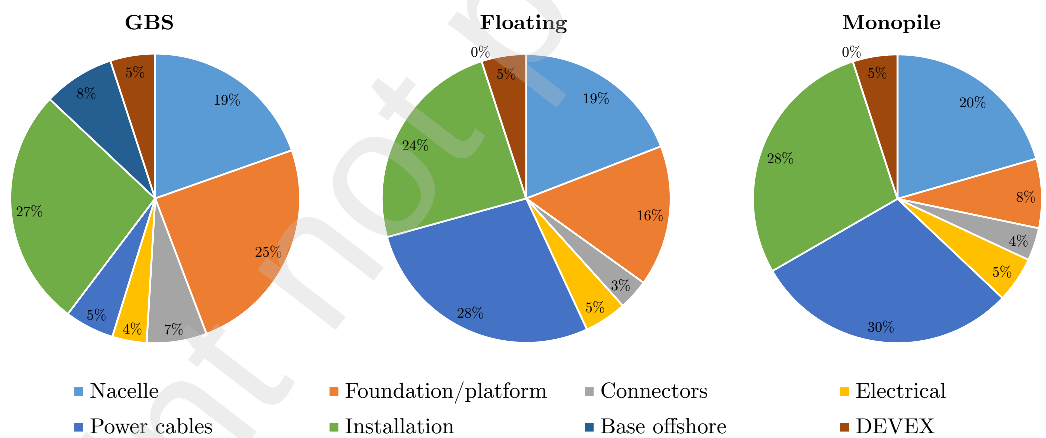

(b) CapEx distribution for 32 TEC array (32 MW) in Raz Blanchard.

Figure 2: Comparison of CapEx distributions for Punta Pezzo and Raz Blanchard sites.

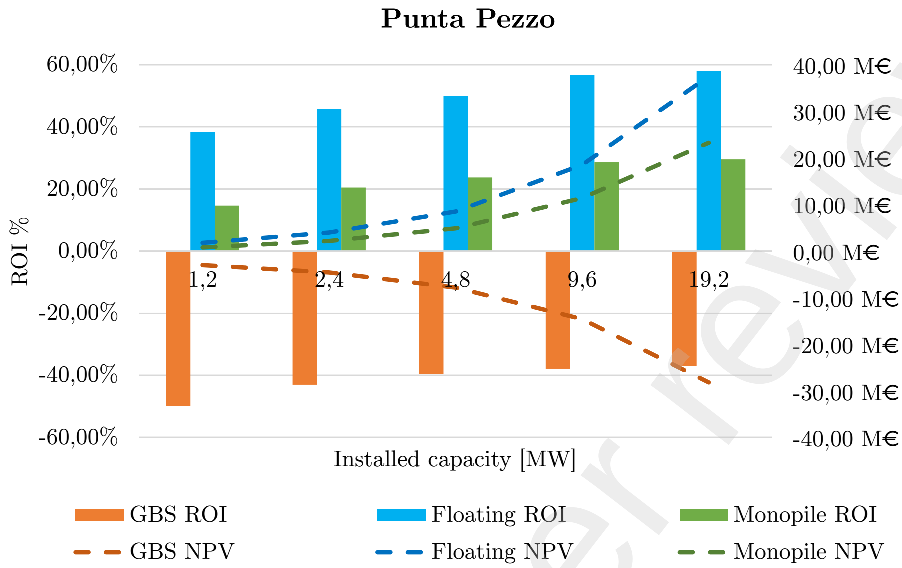

(a) NPV and ROI at different installed capacity and configurations in Punta Pezzo

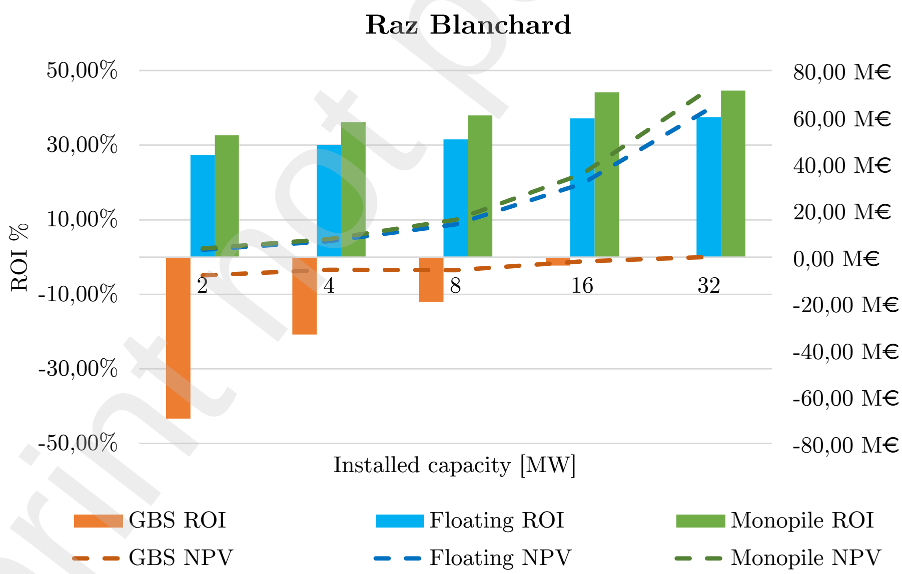

(b) NPV and ROI at different installed capacity and configurations in Raz Blanchard

Figure 3: NPV and ROI as a function of Installed Capacity generated by GBS, Floating, and Monopile TECs in Punta Pezzo and Raz Blanchard. Bars and dashed lines represent ROI and NPV values, respectively.

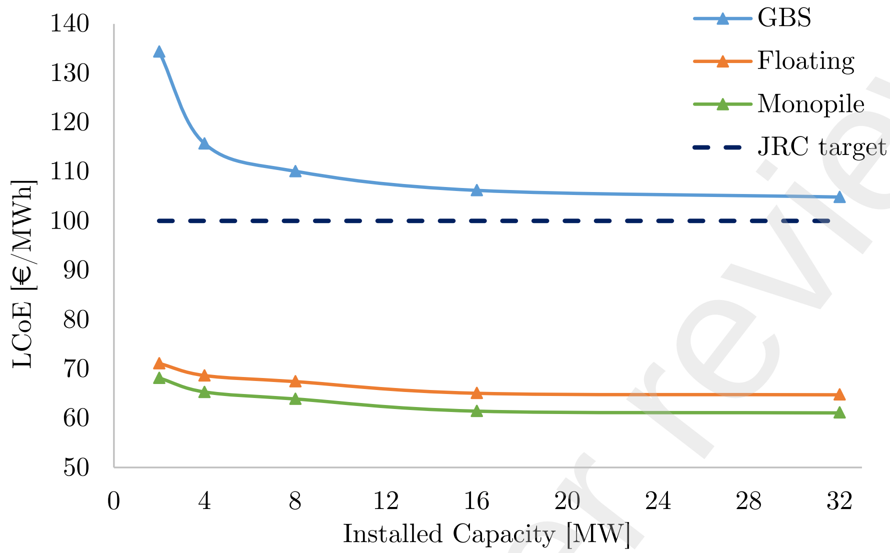

Figure 4: LCoE trends for GBS, floating, and monopile TEC arrays at Fromveur as a function of installed capacity, with JRC target of 100 €/MWh

floating systems generally incur lower OpEx than GBS, although benchmark values diverge due to high OpEx uncertainty [16]. The modeled CapEx for monopiles differs from the 6.8 M€/MW literature value [14], likely influenced by the high-cost assumptions from the Meygen Phase 1C project, which in turn was based on elevated costs from the earlier Phase 1A.

Tidal energy, while offering significant environmental benefits like reduced CO_2 emissions, has notable social and ecological impacts. Socially, community involvement is crucial for project acceptance and can generate local economic benefits [46]. Ecologically, differently from floating WECs [47], tidal turbines can alter ocean hydrodynamics in a way to poses threats to marine wildlife through noise, habitat disruption, and collision risks, and require careful site selection and mitigation. However, innovative turbine designs and the creation of protected offshore zones offer potential solutions to minimize these negative impacts [48].

The environmental advantages of tidal energy, particularly in terms of carbon footprint reduction, must be balanced against potential social and ecological challenges. From a social perspective, successful project implementation depends heavily on community engagement and stakeholder participation, which can simultaneously create opportunities for local economic development [46]. On the ecological front, tidal energy systems may affect marine ecosystems through potential collision risk with turbine blades, disturbance from underwater noise, changes in oceanographic processes, and exposure to electromagnetic fields [49]. These concerns need comprehensive environmental impact assessments and strategic site planning. Nevertheless, advances in turbine technology and the establishment of marine protected areas around installations present viable pathways for impact mitigation [48].

4. Summary and conclusions

This study presented a comprehensive bottom-up (BuA) techno-economic model for evaluating three key tidal energy converter (TEC) configurations, meaning gravity-based substructures (GBS), monopile foundations, and floating platforms, across five distinct coastal sites. By employing detailed, parameterized cost functions derived from industry data and normalized for current economic conditions, the model offers enhanced transparency and flexibility compared to traditional top-down approaches.

The analysis showed that monopile and floating TECs generally achieve better performance in terms of capacity factor and Levelized Cost of Energy (LCoE), especially at sites such as Fall of Warness and Fromveur, where LCoE values dropped below 65 €/MWh. These results meet the European Commission's cost targets for tidal energy. Floating platforms proved most suitable for deep-water locations like Punta Pezzo, while monopile configurations were more cost-effective in shallower waters. GBS systems, although less competitive overall, showed relative advantages in shallow, nearshore sites like Cozumel.

The model was validated against the real-world ATIR floating platform, showing good agreement in terms of capital and operational costs, thus reinforcing the robustness of the proposed methodology. However, further refinements are recommended, particularly for site-specific OpEx estimations and the inclusion of probabilistic failure models to capture uncertainties in marine environments.

Overall, the bottom-up methodology developed here represents a novel and scalable tool to support decision-making in early-stage design and site selection for tidal energy projects. It contributes to the advancement of the economic viability of marine renewables by providing realistic, component-based cost assessments tailored to environmental and technological variability.

Author Contributions

Conceptualization, M.P., E.G.-P., M.C.-G., and G.G.; methodology, M.P., E.G.-P., M.C.-G., and G.G.; software, M.P., E.G.-P., and M.C.-G.; validation, M.P., E.G.-P., and M.C.-G.; formal analysis, M.P., E.G.-P., M.C.-G., and G.G.; investigation, M.P., E.G.-P., M.C.-G., and G.G.; resources, M.P., E.G.-P., M.C.-G., and G.G.; data curation, M.P., E.G.-P., M.C.-G., and G.G.; writing—original draft preparation, E.G.-P., and J.O.-G.; writing—review and editing, M.P., E.G.-P., M.C.-G., and G.G.; visualization, M.P., E.G.-P., and M.C.-G.; supervision, M.P., and E.G.-P.; project administration, E.G.-P., and G.G.; funding acquisition, G.G. All authors have read and agreed to the published version of the manuscript.

Funding

This research was funded by the European Union – NextGenerationEU Award Number: Project code PE0000021, Concession Decree No. 1561 of 11.10.2022 adopted by Ministero dell'Universitá e della Ricerca (MUR), Italy, CUP, Italy E13C22001890001, Project title "Network 4 Energy Sustainable Transition – NEST". Additionally, this project has received funding from the European Union's Horizon Europe Research and Innovation Programme of Blue Energy Offshore Installation Accelerator (Blue-X) under Grant Agreement No 101131527.

Data Availability Statement

The original contributions presented in this study are included in the article. Further inquiries can be directed to the corresponding author.

Acknowledgements

We are grateful to the European Union's Horizon Europe Research and Innovation Programme of Blue Energy Offshore Installation Accelerator (Blue-X) for the funding Grant Agreement No 101131527, the Marine Offshore Renewable Energy Lab (MOREnergy) Lab-DIMEAS (Politecnico di Torino) for supporting this research.

Declaration of competing interest

The authors declare no conflict of interest.

Appendix A. Data of selected tidal sites and turbines

Table A.5: Summary of main characteristics of selected tidal sites and tidal turbines

	Parameter	Fall of Warness	Fromveur	Raz Blanchard	Punta Pezzo	Cozumel
Site location	Latitude	59.14°	48.44°	49.76°	38.23°	20.51°
	Longitude	-2.82°	-5.03°	-2.01°	15.63°	-86.95°
Environmental parameters	Water depth [m]	49	51.3	55	100	19.1
	Distance from shore [m]	1600	2500	11100	600	19.1
Tidal turbine characteristics	Turbine name	Orbital O2	Seagen S-2 MW	Seagen S-2 MW	Seagen S-1.2 MW	Tocardo T2
	Foundation	Floating	Monopile	Monopile	Monopile	Tidal range
	Rotor diameter [m]	20	20	20	16	9.9
	Rated power [kW]	1000	1000	1000	600	103
	Rated current [m/s]	2.65	2.5	2.5	2.35	2
	Cut-in velocity [m/s]	1	1	1	0.7	0.4
	Cut-out velocity [m/s]	4	4	4	4	2.6

Appendix B. Equations

Here's a list of equations of variables/techno-economic parameters involved in this study.

$$AEP = P_{yearly\,mean} \cdot 8760\,, \tag{B.1}$$

$$CF = \frac{P_{yearly\,mean}}{P_{rated}} \tag{B.2}$$

$$F_T = \frac{1}{2}\rho A C_T U^2\,, \quad [50] \tag{B.3}$$

$$\omega_{lss} = \frac{U \cdot TSR}{D/2} \tag{B.4}$$

$$\begin{aligned} N_{elements} = N_{blades} + N_{foundation} + N_{chain\ lines} \\ + N_{anchors} + N_{shackles} \end{aligned} \tag{B.5}$$

$$C_{cable,inst} = 100 \cdot \frac{2}{3} \cdot L + 282 \cdot \frac{1}{3} \cdot L\,, \tag{B.6}$$

$$COST_{2024} = COST_{reference,year} \cdot \frac{CPI_{2024}}{CPI_{reference,year}}, \tag{B.7}$$

$$LCoE = \frac{CapEx + \sum_{t=1}^{n} \frac{OpEx_t}{(1+r)^t} + \frac{D_c}{(1+r)^n}}{\sum_{t=1}^{n} \frac{AEP_t}{(1+r)^t}}\,, \tag{B.8}$$

$$NPV = -CapEx + \sum_{t=1}^{n} \frac{R_t - OpEx_t}{(1+r)^t} + \frac{D_c}{(1+r)^n}\,,\ [12] \tag{B.9}$$

$$R_t = AEP_t \cdot p_{el}\,, \tag{B.10}$$

$$ROI\ [\%] = \frac{NPV}{C_{tot}}\,,\ [51] \tag{B.11}$$

$$C_{tot} = CapEx + \sum_{t=1}^{n} \frac{OpEx_t}{(1+r)^t} + \frac{D_c}{(1+r)^n}\,, \tag{B.12}$$

$$NPV = -CapEx + \sum_{t=1}^{T} \frac{R_t - OpEx_t}{(1+r)^t} = 0\,, \tag{B.13}$$

$$PP = T = \frac{\ln\left(\frac{R-OpEx}{R-OpEx-r\cdot CapEx}\right)}{\ln(1+r)}\,, \tag{B.14}$$

$$E_{CO_2} = EF \cdot AEP\,,\ [40] \tag{B.15}$$

References

[1] J. C. Alcérreca-Huerta, J. I. Encarnacion, S. Ordoñez-Sánchez, M. Callejas-Jiménez, G. Gallegos Diez Barroso, M. Allmark, I. Mariño-Tapia, R. Silva Casarín, T. O'Doherty, C. Johnstone, L. Carrillo, Energy yield assessment from ocean currents in the insular shelf of cozumel island, Journal of Marine Science and Engineering 7 (5) (2019). doi:10.3390/jmse7050147.

[2] A. Russell, J. Firestone, D. Bidwell, M. Gardner, Place meaning and consistency with offshore wind: An island and coastal tale, Renewable and Sustainable Energy Reviews 132 (2020). doi:https://doi.org/10.1016/j.rser.2020.110044.

[3] C. Frost, Quantifying the benefits of tidal stream energy to the wider uk energy system, Tech. rep., Offshore Renewable Energy Catapult (2022). URL https://ore.catapult.org.uk/analysisinsight/quantifying-the-benefits-of-tidal-stream-energy-to-the-wider-uk-energy-system

[4] E. Tapoglou, L. Mc Govern, A. Georgakaki, A. Mountraki, S. Letout, E. Ince, J. Gea Bermudez, A. Schmitz, M. Grabowska, Clean energy technology observatory: Ocean energy in the european union - 2024 status report on technology development, trends, value chains and markets, Tech. rep., Joint Research Centre (2024). doi:10.2760/1244922.

[5] E. Giglio, E. Petracca, B. Paduano, C. Moscoloni, G. Giorgi, S. A. Sirigu, Estimating the cost of wave energy converters at an early design stage: A bottom-up approach, Sustainability 15 (8) (2023). doi:10.3390/su15086756.

[6] E.-B. Konuk, M. Centeno-Telleria, A. Zarketa-Astigarraga, J.-I. Aizpurua, G. Giorgi, G. Bracco, M. Penalba, On the definition of a comprehensive technology-informed accessibility metric for offshore renewable energy site selection, Journal of Marine Science and Engineering 11 (9) (2023). doi:10.3390/jmse11091702.

[7] E. Segura, R. Morales, J. A. Somolinos, Cost assessment methodology and economic viability of tidal energy projects, Energies 10 (11) (2017). doi:10.3390/en10111806.

[8] T. Tan, V. Vengatesan, Enhancing wave resource assessment of high energy sites through wave-current interaction modelling, SSRN Preprint (2025). doi:10.2139/ssrn.5281396.

[9] L. Evans, I. Ashton, B. G. Sellar, Impact on energy yield of varying turbine designs under conditions of misalignment to the current flow, Energies 16 (9) (2023). doi:10.3390/en16093923.

[10] D. Magagna, A. MacGillivray, H. Jeffrey, C. Hanmer, A. Raventos, A. Badcock-Broe, E. Tzimas, Wave and tidal energy strategic technology agenda, Tech. rep., SI Ocean (2014).
URL https://www.policyandinnovationedinburgh.org/wave-and-tidal-energy-strategic-technology-agenda.html

[11] E. Segura, R. Morales, J. Somolinos, A. López, Techno-economic challenges of tidal energy conversion systems: Current status and trends, Renewable and Sustainable Energy Reviews 77 (2017) 536–550. doi:https://doi.org/10.1016/j.rser.2017.04.054.

[12] R. O'Connell, M. Kamidelivand, I. Polydoros, C. Wright, P. Bonar, A. J. Williams, J. Murphy, The integration of tools for the techno-economic evaluation of fixed and floating tidal energy deployment in the irish sea, Energies 16 (22) (2023). doi:10.3390/en16227526.

[13] OffshoreWIND, Scotrenewables secures gbp 7.6 million for tidal energy project (uk), Accessed: 13-01-2025 (2012).
URL https://www.offshorewind.biz/2012/12/14/scotrenewables-secures-gbp-7-6-million-for-tidal-energy-project-uk/

[14] S. Santhakumar, H. Meerman, A. Faaij, Future costs of key emerging offshore renewable energy technologies, Renewable Energy 222 (2024) 119875. doi:https://doi.org/10.1016/j.renene.2023.119875.

[15] A. Iyer, S. Couch, G. Harrison, A. Wallace, Variability and phasing of tidal current energy around the united kingdom, Renewable Energy 51 (2013) 343–357. doi:https://doi.org/10.1016/j.renene.2012.09.017.

[16] M. Bianchi, A. Arnal, M. Astorkiza-Andres, J. Clavell-Diaz, A. Marques, M. Isasa-Sarralde, Life cycle and economic assessment of tidal energy farms in early design phases: Application to a second-generation tidal device, Heliyon 10 (12) (2024). doi:https://doi.org/10.1016/j.heliyon.2024.e32515.

[17] D. Rose, 2024 State of the Science Report - Chapter 7: Education and Outreach Around Environmental Effects of Marine Renewable Energy, Tech. rep., Pacific Northwest National Laboratory (PNNL) (2024). URL https://tethys.pnnl.gov/publications/2024-state-science-report-chapter-7-education-outreach-around-environmental-effects

[18] A. Vargiu, R. Novo, C. Moscoloni, E. Giglio, G. Giorgi, G. Mattiazzo, An energy cost assessment of future energy scenarios: A case study on san pietro island, Energies 15 (13) (2022). doi:10.3390/en15134535.

[19] R. Campbell, A. Martinez, C. Letetrel, A. Rio, Methodology for estimating the french tidal current energy resource, International Journal of Marine Energy 19 (2017) 256–271. doi:https://doi.org/10.1016/j.ijome.2017.07.011.

[20] Ocean Energy Europe, Sabella, [Accessed: 28-09-2025]. URL https://www.oceanenergy-europe.eu/annual/sabella

[21] S. Barbarelli, G. Florio, M. Amelio, N. Scornaienchi, A. Cutrupi, G. Lo Zupone, Design procedure of an innovative turbine with rotors rotating in opposite directions for the exploitation of the tidal currents, Energy 77 (2014) 254–264. doi:https://doi.org/10.1016/j.energy.2014.08.044.

[22] M. Togneri, M. Lewis, S. Neill, I. Masters, Comparison of adcp observations and 3d model simulations of turbulence at a tidal energy site, Renewable Energy 114 (2017) 273–282. doi:https://doi.org/10.1016/j.renene.2017.03.061.

[23] CMDS-EU, Copernicus marine data store, [Accessed: 22-11-2024]. URL https://data.marine.copernicus.eu/products

[24] M. Lewis, S. Neill, P. Robins, M. Hashemi, S. Ward, Characteristics of the velocity profile at tidal-stream energy sites, Renewable Energy 114 (2017) 258–272. doi:https://doi.org/10.1016/j.renene.2017.03.096.

[25] European Climate, Infrastructure and Environment Executive Agency (CINEA), Dtoceanplus—design tools for ocean energy systems innovation, Accessed: 28-09-2025 (2021). URL https://cinea.ec.europa.eu/featured-projects/dtoceanplus_en

[26] F. Balestrino, D. Coiro, G. Giannini, D. Giudice, G. Troise, Resource assessment for the gemstar tidal current energy harvester deployment in the strait of messina, in: 13Th European Wave and Tidal Energy Conference, Naples, Italy, 2019, p. 10. URL https://www.researchgate.net/publication/337275969_Resource_assessment_for_the_GEMSTAR_tidal_current_energy_harvester_deployment_in_the_strait_of_Messina

[27] K. Abed, A. El-Mallah, Capacity factor of wind turbines, Energy 22 (5) (1997) 487–491. doi:https://doi.org/10.1016/S0360-5442(96)00146-6.

[28] L. R. Núñez Rivas, A. López Piñeiro, J. A. Somolinos Sánchez, E. M. Novoa Rojas, A. Carneros Lozano, Comparative analysis of life cycle costs between the 2nd generation tec gesmay ant a 1st generation tec, in: 11Th European Wave and Tidal Energy Conference, Nantes, France, 2015, p. 10. URL https://oa.upm.es/38538/

[29] E. Fernandez-Rodriguez, T. Stallard, P. Stansby, Experimental study of extreme thrust on a tidal stream rotor due to turbulent flow and with

opposing waves, Journal of Fluids and Structures 51 (2014) 354–361. doi:https://doi.org/10.1016/j.jfluidstructs.2014.09.012.

[30] W. Finnegan, E. Fagan, T. Flanagan, A. Doyle, J. Goggins, Operational fatigue loading on tidal turbine blades using computational fluid dynamics, Renewable Energy 152 (2020) 430–440. doi:10.1016/j.renene.2019.12.154.

[31] MetalMiner, Steel Prices & Dynamic Steel Price Forecasting for 2025, Accessed: 17-01-2025.
URL https://agmetalminer.com/metal-prices/carbon-steel/

[32] FocusEconomics, Steel (usa) prices, Accessed: 02-01-2025.
URL https://www.focus-economics.com/commodities/base-metals/steel-usa/

[33] F. Correia da Fonseca, L. Bento do Amaral, M. Rentschler, F. Arede, P. Chainho, Y. Yang, D. Noble, A. Petrov, V. Nava, N. Germain, N. Lariviere-Gillet, J. Henderson, B. Hudson, DTOceanPlus Deliverable D5.7 - Logistics and Marine Operations Tools -Alpha version, Tech. rep., WavEC - Offshore Renewables (2020). doi:10.13140/RG.2.2.34806.61765.

[34] A. Tétu, J. F. Chozas, J. P. Kofoed, Liftwec development of a new class of wave energy converter based on hydrodynamic lift forces deliverable d8.1: Cost database, Tech. rep., Aalborg University (2020).
URL https://liftwec.com/d8-1-cost-database/

[35] M. Kamidelivand, P. Deeney, F. D. McAuliffe, K. Leyne, M. Togneri, J. Murphy, Scenario analysis of cost-effectiveness of maintenance strategies for fixed tidal stream turbines in the atlantic ocean, Journal of Marine Science and Engineering 11 (2023). doi:10.3390/jmse11051046.

[36] Black&Veatch, Lessons Learnt from MeyGen Phase 1A: Final Summary Report, Tech. rep., Department for Business Energy and Industrial Strategy (BEIS) (2020).
URL https://tethys-engineering.pnnl.gov/publications/lessons-learnt-design-installation-initial-operations-phases-\6mw-4-turbine-tidal-array

[37] ARUP, Review of Approaches and Cost of Decommissioning Small Scale Offshore Renewable Energy Developments, Tech. rep., Ove Arup & Partners Ltd (2018).
URL https://consult.gov.scot/marine-scotland/offshore-renewables-decommissioning-guidance/supporting_documents/MSLOT%20small%20scale%20OREI%20decommissioning%20%20Final%20issue.pdf

[38] U.S. Bureau of Labor Statistics, How to Use the Consumer Price Index for Escalation, Accessed: 13-01-2025 (2023).
URL https://www.bls.gov/cpi/factsheets/escalation.htm

[39] Z. Maksumic, Uk awards six tidal stream projects with contracts for difference in allocation round 6, Accessed: 14-01-2025 (2024).
URL https://www.offshore-energy.biz/uk-awards-six-tidal-stream-projects-with-contracts-for-difference-in-allocation-round-6/

[40] M. Corrales-Gonzalez, G. Lavidas, A. Lira-Loarca, G. Besio, Wave energy assessment and wave converter applicability at the pacific coast of central america, Frontiers in Energy Research 12 (2024). doi:10.3389/fenrg.2024.1454275.

[41] M. Renovables, Magallanes renovables.
URL https://www.magallanesrenovables.com/

[42] Magallanes Renovables, Magallanes renovables: Business deck, Accessed: 14-01-2025.
URL https://maritime-forum.ec.europa.eu/document/download/85b06a7e-2ba4-43f4-938d-8f6bca1336c2_en?filename=magallanes_renovables_-_investor_deck_.blueinvest.pdf&prefLang=mt

[43] MeyGen Ltd, MeyGen Tidal Energy Project Phase 1 Environmental Statement, Tech. rep., MeyGen Ltd (2012).
URL https://tethys.pnnl.gov/sites/default/files/publications/MeyGen-2012-ES.pdf

[44] E. marine Energy Centre (EMEC), Magallanes atir project information summary, Tech. rep., European Marine Energy Centre Ltd (EMEC) (2021).

URL https://marine.gov.scot/sites/default/files/project_information_summary_12.pdf

[45] E. González-Gorbeña, A. Pacheco, T. A. Plomaritis, Óscar Ferreira, C. Sequeira, Estimating the optimum size of a tidal array at a multi-inlet system considering environmental and performance constraints, Applied Energy 232 (2018) 292–311. doi:https://doi.org/10.1016/j.apenergy.2018.09.204.

[46] A. Howell, C. Drake, Scoping study on socio-economic impacts of tidal energy development in nova scotia: a research synthesis & priorities for future action, Tech. rep., Nova Scotia Department of Energy & Offshore Energy Environmental Research Association (2012).
URL https://oera.ca/research/scoping-study-socio-economic-impacts-tidal-energy-development-nova-scotia-research

[47] B. Battisti, G. Giorgi, G. V. Fernandez, Balancing power production and coastal protection: A bi-objective analysis of wave energy converters, Renewable Energy 220 (2024). doi:https://doi.org/10.1016/j.renene.2023.119702.

[48] L. Olivia, Artificial reef effect in relation to offshore renewable energy conversion: state of the art, The Scientific World Journal (2012). doi:10.1100/2012/386713.

[49] A. E. Copping, L. G. Hemery, D. M. Overhus, L. Garavelli, M. C. Freeman, J. M. Whiting, A. M. Gorton, H. K. Farr, D. J. Rose, L. G. Tugade, Potential environmental effects of marine renewable energy development—the state of the science, Journal of Marine Science and Engineering 8 (11) (2020). doi:10.3390/jmse8110879.

[50] R. Martin-Short, J. Hill, S. Kramer, A. Avdis, P. Allison, M. Piggott, Tidal resource extraction in the pentland firth, uk: Potential impacts on flow regime and sediment transport in the inner sound of stroma, Renewable Energy 76 (2015) 596–607. doi:https://doi.org/10.1016/j.renene.2014.11.079.

[51] M. H. Nabil, J. Barua, U. R. J. Eiva, M. A. Ullah, T. A. Chowdhury, S. M. S. Siddiquee, M. E. Alam, R. Das, Techno-economic analysis of commercial-scale 15 mw on-grid ground solar pv systems in bakalia: A

feasibility study proposed for bpdb, Energy Nexus 14 (2024). doi: https://doi.org/10.1016/j.nexus.2024.100286.